

Explaining the Visible and Near-Infrared Circular Dichroism Spectra of Light-Harvesting 1 Complexes from Purple Bacteria: A Modeling Study

Sofia Georgakopoulou,[†] Rienk van Grondelle,[†] and Gert van der Zwan^{*‡}

Department of Biophysics and Physics of Complex Systems, Vrije Universiteit, 1081 HV Amsterdam, The Netherlands, and Department of Analytical Chemistry and Applied Spectroscopy, Vrije Universiteit, 1081 HV Amsterdam, The Netherlands

Received: April 7, 2005; In Final Form: December 7, 2005

In this work, we investigate the origin and characteristics of the circular dichroism (CD) spectrum of various light-harvesting 1 (LH1) complexes. The near-infrared (NIR) CD signal of these core antennae is strongly nonconservative, and the nature of this nonconservativity is under examination in this paper. So far, on the basis of the high-resolution structures of LH2, we have been able to model the absorption and CD spectra in the bacteriochlorophyll (BChl) Q_Y and Q_X regions of LH2 (Georgakopoulou et al., *Biophys. J.* **2002**, *82*, 2184–2197), as well as in the carotenoid region (Georgakopoulou et al., *Biophys. J.* **2004**, *87*, 3010–3022). We proceed by applying the same modeling method in order to reproduce the LH1 spectra. We assume a ring of dimers in a perfect circular arrangement with 16-fold symmetry, and account for all excitonic interactions within the ring. Because LH1 complexes exhibit Q_Y and Q_X CD signals of very low intensity, higher transitions can easily affect these regions. Therefore, we expand the model and take into account also the Soret and carotenoid transitions. We can now understand the shape of the absorption and CD spectra and contemplate the structure of the LH1 complex. The latter is similar to LH2 in that it is a very symmetric ring dominated by excitonic interactions. The larger number of symmetry and the bigger diameter of LH1, combined with small rotations of the BChl transition dipole moments, are responsible for the display of CD signals that are very low in intensity. The interaction of the Q_Y with the carotenoid transitions results in complete loss of the conservativity. Interaction energies between all the pigments in the ring are calculated, and their values are in good accordance with what is reported in the literature.

Introduction

Photosynthetic organisms (plants, algae and bacteria) contain two types of pigment–protein complexes: light-harvesting (LH) complexes and reaction centers (RC). The LH complexes capture the light and transfer it to the RC, where a series of dark electron-transfer reactions occur, leading to the creation of an electrochemical potential.^{1–5} For purple bacteria, the photosynthetic unit is very well characterized and the structures of several bacterial pigment–protein complexes are known to high resolutions.^{6–12} Especially for the LH2 (peripheral) antenna complexes that exhibit highly symmetrical rings of pigments, numerous calculations of their intermolecular interactions and of their spectroscopic features have been performed.^{5,13–18}

In this study, we attempt a modeling of the absorption and circular dichroism (CD) spectra of the LH1 (core) antenna, using as a reference point the measured spectra of *Rhodobacter (Rba.) sphaeroides* and *Rhodospirillum (Rsp.) rubrum* LH1 complexes. Although we lack a detailed structure of these complexes, we still have plenty of information arising from several high-resolution LH2 structures, as well as from LH1 structures of lower resolution;^{7–9,11,12} on the basis of these structures, we can make relatively safe assumptions for constructing a working model. We thus wish to investigate several aspects of the

functionality and structure of the LH1 complex in relation to the experimentally obtained spectroscopic properties. In our modeling, we assume a perfect circular arrangement and we take into account interactions between all the pigments of the LH1 ring, bacteriochlorophylls (BChls) and carotenoids. Subsequently, we compare our results to the absorption and CD spectra obtained for several mutants from the aforementioned organisms. Our goal is to understand how the interactions between BChls and carotenoids affect the spectroscopic properties of LH complexes and, specifically, to shed light on the origin of the small and nonconservative Q_Y CD signal of the LH1 complex. The modeling approach that we are using for this purpose has already been applied successfully in the past. In 1997, Koolhaas et al.¹⁹ modeled the absorption and CD spectra of the LH2 complex of *Rhodopseudomonas (Rps.) acidophila*, giving a very good description of the red-shift of the zero crossing in the CD signal. Later, Koolhaas et al.²⁰ identified and characterized precisely the upper exciton component of the B850 band of purple bacteria LH2 by means of absorption and CD spectroscopy and modeling on mutants of *Rba. sphaeroides* that lacked the B800 band. This study provided an accurate estimate for the strength of the nearest-neighbor interaction between the BChls Q_Y in the LH2 ring of about 300 cm⁻¹. This number was fully consistent with the long time pump–probe spectrum,^{21,22} the superradiance of LH2,²³ and quantum chemical calculations.¹⁵ We should note that, in that case, the known *acidophila* LH2 structure was used to simulate the B850 ring of *Rba. sphaeroides* LH2. Similarly, in Georgakopoulou et al.,²⁴

* Corresponding author. E-mail: zwan@chem.vu.nl.

[†] Department of Biophysics and Physics of Complex Systems, Vrije Universiteit.

[‡] Department of Analytical Chemistry and Applied Spectroscopy, Vrije Universiteit.

we used the known structures of *Rps. acidophila* and *Rsp. molischianum* LH2 to model the absorption and CD spectra of a variety of LH2 complexes by categorizing them into two groups: the acidophila-like, and the molischianum-like LH2s.²⁴ Recently, by using again the two known structures, we reproduced with great precision the absorption and CD spectra of the carotenoid region in the LH2 complexes of *Rps. acidophila* and *Rsp. molischianum*. By combining the results of these two studies, we are able to acquire an accurate picture of the positions and orientations of the pigments' transition dipole moments in the ring.

So far, the available structures of LH1 complexes are not sufficiently elucidative to give a detailed account of the positions of the pigments. Many studies proposing different geometries and organizations for various LH1 rings are currently available,^{25–29} but none of them provides the accuracy needed for a confident assignment of all the molecules in these structures. Besides, we lack a detailed structural model for the LH1 of *Rba. sphaeroides*; it is, however, safe to postulate that it is a hexadecamer just like the *Rsp. rubrum* LH1.⁷ Such an assumption has been made in the past by Hu and Schulten³⁰ for modeling the atomic structure of the entire *Rba. sphaeroides* LH1 antenna; with their modeling, they demonstrated that 16 is the smallest number of $\alpha\beta$ -heterodimers needed to form a circular ring around the reaction center (RC). More recently, the RC-LH1 structure from *Rps. palustris* was revealed at higher resolution.¹¹ This LH1 ring contains 15 dimers, and a single protein is located in an opening of the ring, where a 16th dimer could fit. Our modeling has shown that accounting for pigments that are half a ring apart is the minimum requirement for reproducing the measured absorption and CD spectra.^{19,31} However, one missing dimer in the ring does not affect the spectra significantly (see Results Section and Figure 4B). Besides, as we have seen in a previous modeling study on the absorption and CD spectra of several LH2 complexes,²⁴ a small change in the symmetry number (the number of times the basic building block of the structure needs to be repeated to give the final ring) does not affect the shape of the spectra and the modeling parameters in a very significant way and should generally not create any problems in the interpretation of the results. Another assumption we make for creating a trustworthy LH1 ring is that it is a ring of structural dimers. This is a reasonable statement because it is well-known that LH1 has the tendency to break into dimers when solubilized in detergent or when heated, and it is reconstituted as soon as normal conditions are reestablished.^{31–33} Finally, because of the high homology in the amino acid sequences of the apoproteins in the LH2 complex of *Rsp. molischianum* and the LH1 complexes of purple bacteria,³⁴ we can safely accept that the LH1 ring resembles a lot the B850 ring of the *Rsp. molischianum* LH2 antenna, and therefore, we use the latter structure as the starting point for our modeling. All the assumptions made above are essential for continuing with the calculation of the absorption and CD spectra, and although they are not based on a real structure, there is still strong evidence supporting them.

Computational Methods

The modeling program we use for calculating the absorption and CD spectra has been described several times in previous papers.^{19,20,24,35–38} Here, we will only give a short description of the whole concept of this modeling, the logical structure of the computer program, and some basic theoretical background.

The first step in the modeling procedure is to create a model LH1 ring. For this purpose, we need the positions and directions

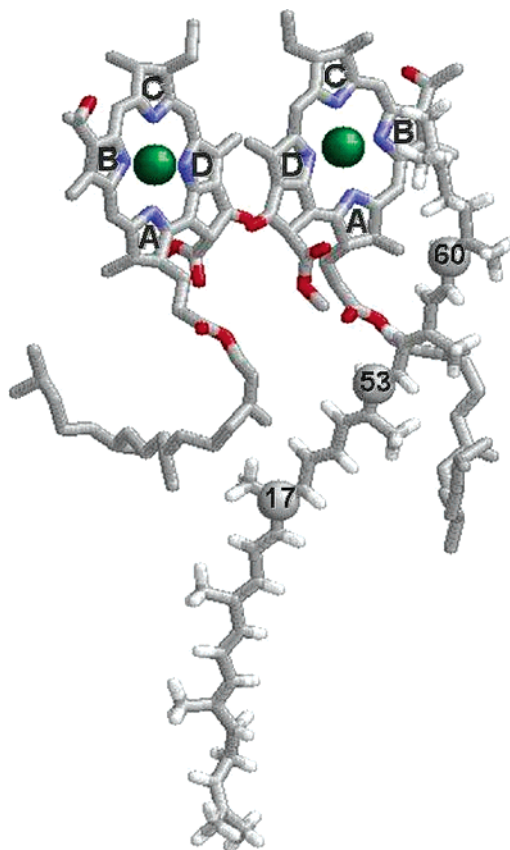


Figure 1. Basic building block of *Rsp. molischianum* LH2 antenna, used as a starting point for creating the modeled LH1 complex and the positions and directions of the transition dipole moments in it. In green, the magnesium (Mg) atoms are shown. In blue are the nitrogens (N) numbered according to the corresponding pyrrole ring; N_A – N_C denotes the X direction, while N_B – N_D denotes the Y direction of the BChls transition dipole moments. The carotenoid transition dipole moment is along the C_{17} – C_{60} direction, while the center of the carotenoids is indicated by C_{53} .

of all transition dipole moments. We start by constructing the ring of BChls; the magnesium and nitrogen atom coordinates are taken from the first dimer of the *Rsp. molischianum* LH2 structure (1KZU, Brookhaven Protein Data Bank) (Figure 1). After making the necessary adjustments for establishing the correct ring size (in this case two times the size of the molischianum ring), we create a circular ring by rotating each BChl according to the rotation matrix:

$$R = \begin{pmatrix} \cos(i-1)\frac{2\pi}{N} & -\sin(i-1)\frac{2\pi}{N} & 0 \\ \sin(i-1)\frac{2\pi}{N} & \cos(i-1)\frac{2\pi}{N} & 0 \\ 0 & 0 & 1 \end{pmatrix} \quad (1)$$

where N is the size of the symmetry, in this case 16, and i runs from 1 to N . The distances between the BChls in this LH1 ring are the same as for *Rsp. molischianum* LH2; between the α - and β -BChls within a dimer, it is 9.4 Å, while between two dimers (the β -BChl of the first and the α -BChl of the neighboring), the distance is 8.8 Å. These values are in general agreement with calculations of Hu and Schulten³⁰ for a model LH1 ring from *Rba. sphaeroides*. The main difference is that their ring is much more symmetric, with a difference of only 0.1 Å in the BChl distances between neighboring dimers and within one dimer; moreover, the latter distance is also the larger one. The α - and β -BChls are attributed four transition dipole

moments each that account for the Q_Y , Q_X , and Soret (B_Y , B_X) bands. The Q_Y and B_Y transitions are oriented along the N_B-N_D direction of the BChl chlorin ring, and the Q_X and B_X transitions are oriented along the N_A-N_C direction. The possibility of rotating the transition dipole moments around the BChls' z-axis (i.e., perpendicular to the pigment's chlorin plane) is introduced to account for the fact that, in reality, they do not precisely follow the N_B-N_D and N_A-N_C directions, but they may be several degrees off.^{24,39} Moreover, the α - and β -BChls are distinct in terms of site energies and magnitudes of their transition dipole moments.

Subsequently, the carotenoids are introduced. The positions of the carotenoids in the LH1 ring are constructed by acquiring the coordinates of the central carbon atom of one lycopene from the *Rsp. molischianum* LH2 structure (in this case, carbon atom C₅₃, as denoted in the 1KZU structure in the Brookhaven Protein Data Bank). Therefore, the basic building block of the LH1 ring is now one BChl dimer and one carotenoid molecule, and it is defined according to the 1KZU structure: the BChls and carotenoid that belong to the same group form one building block. We proceed by rotating according to eq 1, again after making the necessary adjustments to obtain the correct ring size. The transition dipole moment of the carotenoid is along the line connecting the C₁₇ and C₆₀ carbon atoms from the same structure^{35,40} (Figure 1); these are also rotated according to eq 1 to obtain the dipole moments of all 16 carotenoids of the ring. In this paper, a simplified approach is adopted for modeling the absorption and CD spectra of the carotenoid region, compared to the one used in Georgakopoulou et al., 2004.³⁵ The carotenoid bands are calculated assuming four transitions per carotenoid, one for each vibrational mode of the S_2 ($1B_u^-$) level, and no distinction between the C–C and C=C stretches. The dipole moment and Franck–Condon (FC) factors are estimated empirically and are adjusted so that they give rise to absorption bands with magnitude ratios that correspond with the ones observed experimentally. This gives satisfactory results in terms of line shapes and intensities, as pointed out in Georgakopoulou et al., 2004,³⁵ and serves its purpose without loading the modeling procedure too much, making it too slow and difficult to use.

We can now look at the LH1 ring as l interacting circular rings of $N = 16$ two-level systems each, where l is the number of transition dipole moments belonging to different pigments. In the case that we are dealing with, a ring of α - and β -BChls, $l = 8$, whereas, when we add the carotenoid, transitions l becomes equal to 12. The total Hamiltonian of such a system is the sum of the interaction between pigments m and n of ring γ and the interaction between m and n between two rings, denoted here as γ and $\bar{\gamma}$.

$$H = \sum_{\gamma}^l \sum_n^N ([E_{\gamma}|n_{\gamma}\rangle\langle n_{\gamma}| + \sum_m^N V_{\gamma}|n_{\gamma}\rangle\langle m_{\gamma}|] + \sum_{\bar{\gamma}}^l \sum_m^N V_{\gamma\bar{\gamma}}|n_{\gamma}\rangle\langle m_{\bar{\gamma}}|) \quad (2)$$

where E is the site energy of each different transition, and V is the interaction operator between two pigments, calculated in the point dipole approximation:

$$V = \frac{1}{4\pi\epsilon_0\epsilon_r r_{nm}^3} \vec{\mu}_m \cdot \left(1 - 3\frac{\vec{r}_{nm}\vec{r}_{nm}}{r_{nm}^2}\right) \cdot \vec{\mu}_n \quad (3)$$

Here, r_{nm} is the distance between pigments m and n , $\vec{\mu}_m$ and $\vec{\mu}_n$

are the transition dipole moments, and ϵ_0 and ϵ are the dielectric constant in a vacuum and in the medium. By diagonalizing the Hamiltonian, we get the excitonic states $|k\rangle$ as linear combinations of the pigment electronic states:

$$|\psi_{k,\gamma}\rangle = \sum_{\gamma}^l \sum_m^N C_m^{k\gamma} |m_{\gamma}\rangle \quad (4)$$

where the coefficients $C_m^{k\gamma}$ are the components of the eigenvectors of the Hamiltonian. We can now calculate the absorption and CD spectra as a function of the frequency ν according to:

$$I(\nu) = \frac{2\pi\nu}{3} \text{Im} \sum_{n,m}^N F_{n,m}(\nu) \vec{\mu}_n \cdot \vec{\mu}_m \quad (5)$$

$$R(\nu) = \frac{-16\pi^2\nu}{9\lambda} \text{Im} \sum_{m,n}^N F_{n,m}(\nu) (\vec{\mu}_n \times \vec{\mu}_m) \cdot \vec{r}_{nm} \quad (6)$$

Here, $F_{n,m}(\nu)$ are the coherence correlation functions:

$$F_{n,m}(\nu) = \sum_{\gamma,\bar{\gamma}}^l \langle G(\nu - \nu_{0l}) C_n^{k\gamma} C_m^{k\bar{\gamma}} \rangle \quad (7)$$

where $\langle \rangle$ reflects the averaging procedure, and ν_{0l} is the frequency corresponding to the transition between excitonic levels 0 and l . This expression contains the line shape function, in this case, a Gaussian that simulates homogeneous broadening (σ_{hom}) at every frequency ν . This is a good approximation because, at relatively high temperatures, the fast fluctuations in the medium that couple to the electronic transitions give rise to Gaussian shapes:⁴¹

$$G(\nu - \nu_{0l}) = \frac{1}{\sigma_{\text{hom}}\sqrt{2\pi}} e^{-(\nu - \nu_{0l})^2/\sigma_{\text{hom}}^2} \quad (8)$$

The frequencies ν_l are equal to the energy eigenvalues of the system, divided by $2\pi h$. Inhomogeneous broadening is also taken into account by adding a random contribution to the diagonal elements of the Hamiltonian system:

$$H_r = \sum_m \Delta_m |m\rangle\langle m| \quad (9)$$

Results

The CD spectra of the WT LH1 antennae from *Rba. sphaeroides* and *Rsp. rubrum* differ from typical CD spectra from other ring structures (i.e., LH2²⁴) in the lack of conservativity of their Q_Y regions.^{32,42–44} These rather unusual CD signals led to the need to model the absorption and CD spectra and provide some explanation for their origin. Initially, the modeling procedure used in order to calculate these CD spectra involved only the BChl Q_Y and Q_X regions and was along the same lines as those used for modeling the LH2 BChl regions.²⁴ The program was modified so that from the positions of one B850 dimer, derived from the known structure of the *Rsp. molischianum* LH2 complex, a larger ring was created, this time with 16-fold symmetry. The calculated CD spectrum of such a system was similar to that of the LH2 B850 ring and completely conservative as expected for an excitonic CD signal (Figure 2). The parameters used for calculating the spectrum presented here are listed in Table 1; for this case, the parameters concerning the Soret region should be discarded. Very quickly, it became obvious that higher transitions needed to be accounted

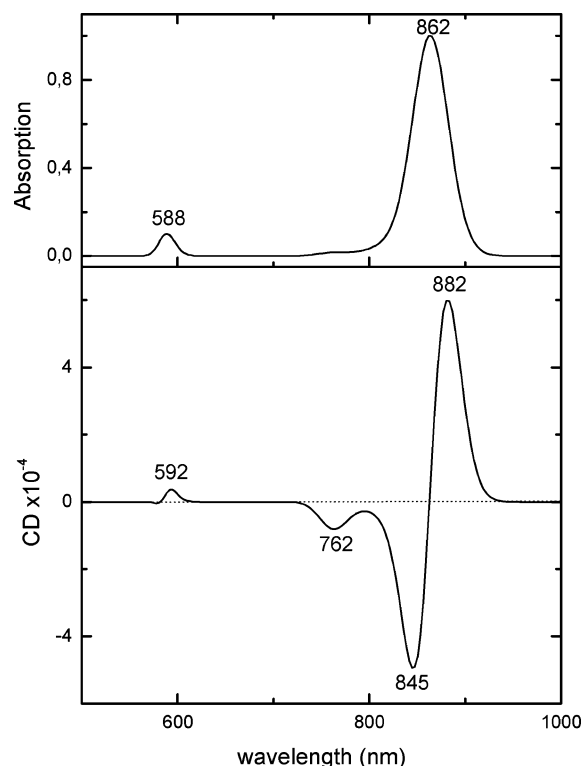


Figure 2. Modeled absorption (top) and CD (bottom) spectra of a BChl ring with 16-fold symmetry; only the Q_Y and Q_X transitions are taken into account. Modeling parameters that lead to these spectra are listed in Table 1.

TABLE 1: Parameters Used for the Calculation of the Absorption and CD Spectra of a Carotenoidless LH1 Ring

	Q_Y		Q_X		B_Y		B_X	
	α	β	α	β	α	β	α	β
μ (Debye)	6.1	7.3	1.6	2.4	9.5	9.8	-10.7	-10.3
E (nm)	803		590		375		375	
ΔE (cm $^{-1}$)	350		-30		1330		1510	
ϵ				1.35				
Δ (cm $^{-1}$)	500		300		1700		1700	
σ (cm $^{-1}$)	600		500		1900		1900	
$\theta(z)$ (deg)	0.2	7.1	-15.0	15.0	5.0	7.0	-10.0	10.0

α , β : α -bound and β -bound BChls; μ : transition dipole moment; E : site energy; ΔE : energy difference between α - and β -BChls; ϵ : dielectric constant; Δ : homogeneous broadening; σ : inhomogeneous broadening; $\theta(z)$: rotation around the pigment z -axis for BChls, z -axis is the axis perpendicular to the chlorin ring; minus sign denotes anticlockwise rotation.

for, which will destroy the conservativity of the near-infrared (NIR) CD signals.

We proceeded by taking into account the higher transitions of the BChls, the Soret (or B) transitions. It was immediately observed that the B_Y and B_X transition dipole moments affect the red part of the spectrum in different ways: the B_Y transition shifts the position of the Q_Y bands to the red both in the absorption and the CD spectra, while the B_X transition is responsible for changes in the shape of the CD signal and hardly affects the NIR absorption. To examine the correctness of our results, we compared them with a mutant of *Rba. sphaeroides* LH1, called here WTW, which contains phytoene instead of the WT spheroidene/spheroidenone mixture of carotenoids (see companion paper).⁴⁴ When we take into account the Soret region in the modeling procedure, we can produce spectra that are in reasonable agreement with the measurements on WTW (Figure 3). The CD signal in the Q_Y region remains mainly conservative,

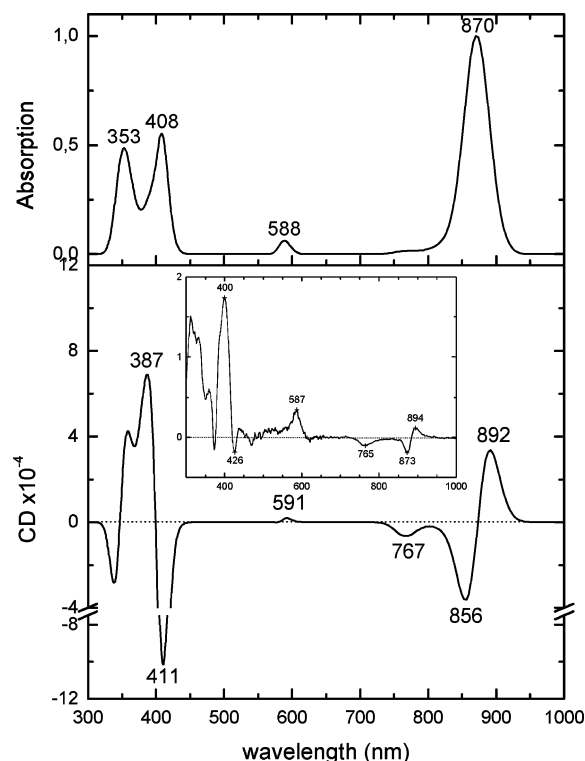


Figure 3. Modeled absorption (top) and CD (bottom) spectra of a BChl ring with 16-fold symmetry. The interacting transition dipole moments are BChls' Q_Y , Q_X and Soret (B_Y and B_X). The parameters used for the modeling are listed in Table 1. The insert shows the measured CD signal of a mutant from *Rba. sphaeroides* LH1 (WTW), which contains the carotenoid precursor phytoene. For more details on measured spectra, see companion paper.⁴⁴

TABLE 2: Interaction Energies (in cm $^{-1}$) between α - and β -BChls

		α -BChl							
		intradimer				interdimer			
		Q_Y	Q_X	B_Y	B_X	Q_Y	Q_X	B_Y	B_X
β -BChl	Q_Y	339	-34	531	182	332	-26	516	125
	Q_X	22	15	26	-103	13	20	9	-137
	B_Y	455	-46	713	244	445	-35	692	168
	B_X	-54	-67	-46	466	-15	-89	25	609

and a negative high exciton band is visible at 767 nm. The parameters used for achieving these results are listed in Table 1. The calculated interaction energy (E_{int}) between the Q_Y transitions of α - and β -BChls within a dimer is 339 cm $^{-1}$, while between two dimers it is 332 cm $^{-1}$, in very good agreement with what has been proposed for LH2.^{5,13-15,20,22-24,45-47} In Table 2, all the intra- and interdimer interaction energies are listed. It can be observed that, for the Y dipoles, the intradimer interactions are larger than the interdimer, while for the X dipoles, the opposite is true. Such trends have been reported before in literature.^{16,17}

Subsequently, the carotenoid transitions were added to the model, as described in the Materials and Methods Section. The carotenoid transition dipole moment was given a value of 7.9 D, and the assigned site energies for the bands were 550 nm, 512, 480, and 450 nm (Table 3) in accordance with the measured spectra of WT *Rba. sphaeroides* and *Rsp. rubrum*. Without changing any other of the parameters listed in Table 1, we observe a drastic change in the shape of the Q_Y CD signal, which becomes negative and is now almost identical with the measured NIR CD of WT LH1 from *Rba. sphaeroides* (Figure 4A). The carotenoid transition dipole moments interact rather strongly

TABLE 3: Parameters Used for the Modeling of the Carotenoid Region of LH1 Complexes Containing Both BChls and Carotenoids^a

	carotenoids			
	WT-like (neurosporene-like)			
	0-0	0-1	0-2	0-3
μ (Debye)	7.9 (6.9)	$\times 1.05$	$\times 0.9$	$\times 0.55$
E (nm)	545 (480)	512 (450)	483 (425)	456 (410)
ϵ			1.35	
Δ (cm ⁻¹)			900	
σ (cm ⁻¹)			1100	
$\theta(z)$ (deg)			-5.0	

^a The parameters used for the BChls are the same as in Table 1. 0-0, 0-1, 0-2, 0-3: vibrational levels of the carotenoids. \times : Franck-Condon factors for the higher vibrational levels; the transition dipole moment of 0-0 is multiplied by the FC factors to give the dipole moments of the higher levels. $\theta(z)$: rotation around the pigment z -axis; for carotenoids, z -axis is the axis perpendicular to the plane defined by the transition dipole moment vector and the long axis of the carotenoid, minus sign denotes anticlockwise rotation. All other symbols denote the same parameters as in Table 1. The values for the neurosporene-like carotenoids are given in parentheses. The parameters used for the BChls are the same as in Table 1.

with the Q_Y transitions of the BChls that belong to the neighboring building block. In particular, the 0th vibrational mode has an interaction energy of 76 cm⁻¹ with the Q_Y transition of the neighboring β -Bchl, while with the one that belongs to the same building block, $E_{\text{int}} = 52$ cm⁻¹. In total, all four carotenoid transitions interact with the neighboring β -Bchl Q_Y , with an energy that adds up to 266 cm⁻¹. In Table 4, the calculated interaction energies between carotenoids and BChls are listed. The strong interaction between the carotenoid transitions of one building block and the Bchl transitions of the next is eminent. Both within one building block and between two neighboring ones, the major contributions to the carotenoid-Bchl interaction come from the X dipoles of the α -BChls and the Y dipoles of the β -BChls. These trends are in agreement with the couplings between the pigments in the *Rsp. molischianum* LH2 complex, calculated by Tretiak et al.,¹⁶ although the actual values do not coincide. However, the differences are not too large, especially in the case of interactions of the carotenoids with the Q dipoles. Taking into account that we are dealing with an LH1 complex for which we have assumed different orientations for the pigments compared to

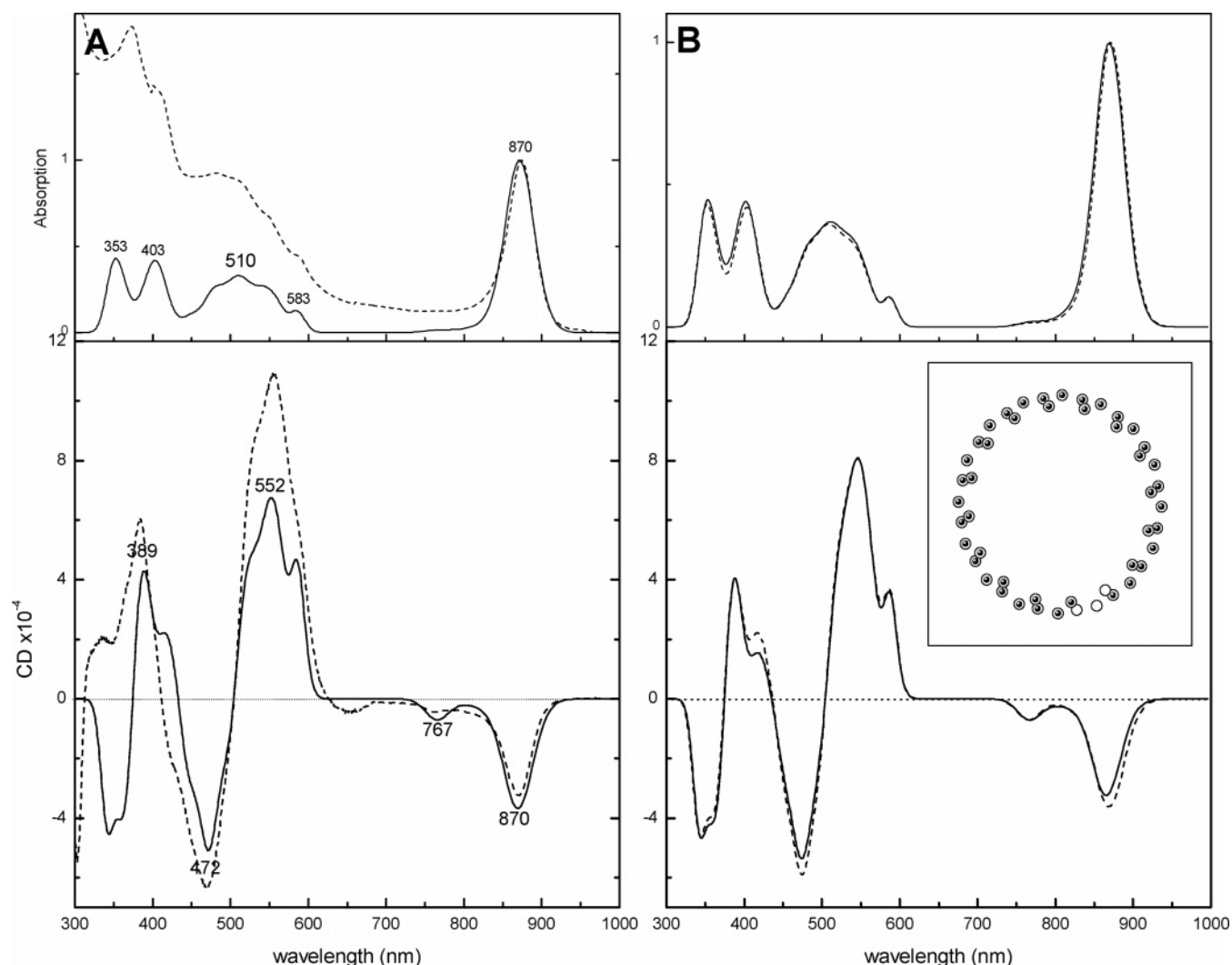


Figure 4. A: Modeled (solid) and measured (dashed) absorption (top) and CD (bottom) spectra of a LH1 ring with 16-fold symmetry that contains both the Bchl (Q_Y , Q_X) and Soret (B_Y and B_X) transitions and the carotenoid transitions ($S_0 \rightarrow S_2$). The measured spectra from *Rba. sphaeroides* WT LH1 contain a mixture of carotenoids (spheroidene/spheroidenone). The absorption spectra are normalized on the Q_Y band, and the CD spectra are scaled on the normalized absorption. For more details on measured spectra, see companion paper.⁴⁴ B: Modeled absorption (top) and CD (bottom) spectra of a LH1 ring with 15 building blocks (solid), simulating a LH1 ring that is missing one Bchl pair and one carotenoid and with 16 building blocks (dashed), simulating a closed LH1 ring. The insert shows a two-dimensional picture of the positions of the pigments in an open ring structure (in black balls) and in a closed ring structure (in white circles). The outer ring shows the centers of the BChls, and the inner ring, the centers of the carotenoids. The parameters used for the modeling for both A and B are listed in Tables 1 and 3.

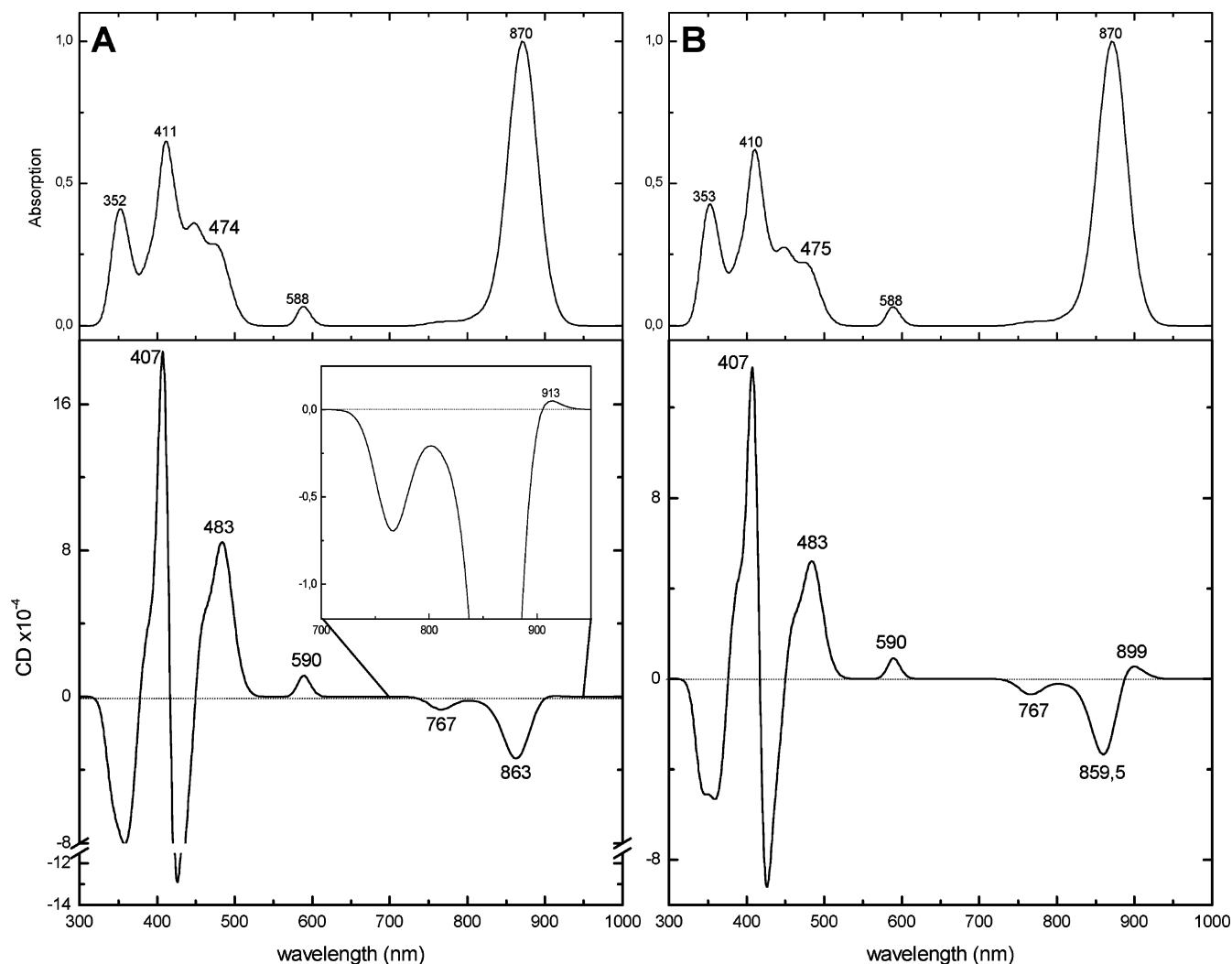


Figure 5. Modeled absorption (top) and CD (bottom) spectra of a LH1 ring with 16-fold symmetry that contains BChl (Q_Y , Q_X , and Soret) and carotenoid ($S_0 \rightarrow S_2$) transitions. The carotenoid site energies are blue-shifted compared to Figure 4 to simulate the different carotenoid (neurosporene). A: Only the site energies are blue-shifted; the insert shows a blow-up of the red part of the modeled Q_Y CD signal. B: The site energies are blue-shifted, and the transition dipole moment is decreased to 6.9 D. The parameters used for the modeling are listed in Tables 1 and 3.

TABLE 4: Interaction Energies (in cm^{-1}) between Carotenoids and BChls

		BChls															
		same building block								neighboring building block							
		α -BChls				β -BChls				α -BChls				β -BChls			
		Q _Y	Q _X	B _Y	B _X	Q _Y	Q _X	B _Y	B _X	Q _Y	Q _X	B _Y	B _X	Q _Y	Q _X	B _Y	B _X
carotenoids	0-0	-4	5	-9	-35	52	-0.2	70	7	16.5	-45	49	303	-76	-19	-102	73
	0-1	-4.5	5.5	-10	-37	55	-0.2	73	7.5	17	-47	52	318	-80	-20	-107	76
	0-2	-4	5	-8.5	-31	47	-0.15	63	6.5	15	-40	44	273	-68	-17	-92	65
	0-3	-2.5	3	-5	-19	29	-0.1	38	4	9	-25	27	167	-42	-10	-56	40

LH2, these discrepancies can be explained. As far as the B dipoles are concerned, in Tretiak et al.,¹⁶ there are more transitions taken into account that absorb in blue the part of the spectrum than just the Soret transitions, therefore, we expect bigger differences.

Next, we examine the effect of open rings in the CD spectra (Figure 4B). We do that by simply removing one building block, consisting of one BChl dimer and one carotenoid, from the circular ring (see insert of Figure 4B). We observed very small changes in both the absorption and the CD spectra. In the Q_Y region, the CD signal becomes slightly smaller in magnitude, and there is a small shift to the blue of approximately 2 nm; however, the completely nonconservative nature of the signal is preserved. In the other parts of the spectra, again, only minor

changes are observed that involve variations only in the magnitude and not in the shape of the signals.

The effect of the carotenoids on the NIR CD signal is tested once more by modeling the absorption and CD spectra of a ring containing carotenoids with chains of shorter conjugation, like the neurosporene-containing LH1 mutants of *Rba. sphaeroides* and *Rsp. rubrum* (see companion paper).⁴⁴ These present Q_Y CD signals that are nonconservative, but to a lesser extent. The absorption and CD spectra calculated for the case of LH1 rings with smaller carotenoids, like the ones described above, are presented in Figure 5A. Here, the carotenoids are positioned more to the blue and the initial positions of the vibrational bands are listed in Table 3; again, all other parameters are kept constant. The modeled Q_Y CD signal is still nonconservative,

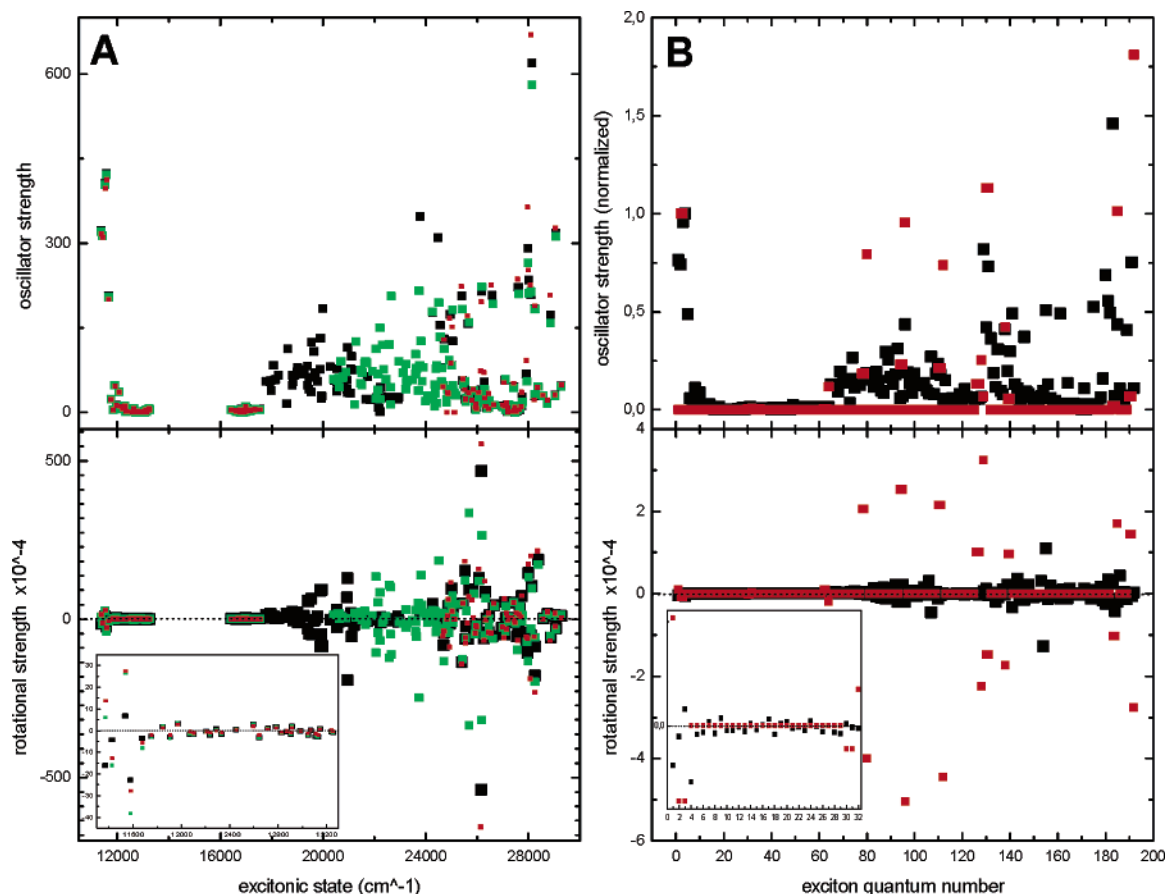


Figure 6. A: Oscillator and rotational strength of the three cases studied; WT-like (black), neurosporene-like (green), and phytoene-like (red). B: Oscillator and rotational strength for the WT-like calculation, with (black) and without (red) inhomogeneous broadening. In this case, the oscillator strengths are normalized, and the rotational strengths are scaled on the relative oscillator strengths. In both A and B, the insert shows the population of the lower (Q_Y) states.

however, it possesses now a small, but distinct positive feature on the red side. If we decrease the dipole moment value of the carotenoid from 7.9 D to 6.9 D, this positive feature becomes more intense (Figure 5B). These results correspond very well with what is observed experimentally, i.e., shorter and, therefore, “bluer” carotenoids affect the conservativity of the Q_Y CD signal less. This is illustrated clearly in Figure 6A, where the oscillator and rotational strength per state, for the three cases described above, are plotted. If we look at the lower states, we notice immediately that there is a high asymmetry in the rotational strength of the WT-like complex, which decreases when we are simulating the neurosporene-containing complex and it disappears when no carotenoids are taken into account. The oscillator strength in the region is not affected. Next, we show a diagram comparing the results for the WT-like calculations with and without inhomogeneity (Figure 6B). We can see now how the states are mixing in the presence of disorder. Note that, without inhomogeneous broadening, the results are in agreement with the findings of Koolhaas et al. for the oscillator and rotational strength of a ring with 9-fold symmetry.¹⁹

We should point out here that, in these models, we adjust the carotenoid transition dipole moments and site energies according to the carotenoids found in our sample each time. It is known that, according to the length of the π -electron chain of the carotenoid, its absorption shifts to the blue (for shorter lengths of conjugation) or to the red (for longer conjugation lengths).⁴⁸ In our modeling, for calculating the WT spectra, we assume a carotenoid dipole moment of 7.9 D and rather red-shifted site energies. This is in agreement with the carotenoids

spheroidene/spheroidenone (and their BChl/carotenoid ratio of 1:1) and spirilloxanthin (with BChl/carotenoid ratio of 2:1) that are found in WT *Rba. sphaeroides* and *Rsp. rubrum*, respectively. The carotenoids in *Rba. sphaeroides* have 10 and 11 conjugated double bonds, and when in solution, they absorb much more to the blue than spirilloxanthin, the 13-double-bond carotenoid of *Rsp. rubrum*. However, probably because of carotenoid–protein interactions, in *Rba. sphaeroides*, these bands are as red-shifted as the ones in *Rsp. rubrum*; moreover, considering the high carotenoid content in *Rba. sphaeroides*, compared to the 2:1 BChl/carotenoid ratio used in our modeling, it is safe to assume an increased transition dipole moment during the modeling procedure that will make up for this discrepancy. Subsequently, for modeling the spectra of the neurosporene-containing complexes, we assume bluer site energies. These values are in accordance with the site energies used for modeling the carotenoids in LH2 of *Rps. acidophila* and *Rsp. molischianum* in an earlier study.⁴⁰ The latter contains carotenoids with 11 conjugated double bonds, and their site energies lie between the values given for the WT and mutant LH1 complexes described above.

The last question we wish to answer is how the aggregation of LH complexes affects their absorption and CD signals. For this purpose, we create four interacting rings of α - and β -BChls, arranged around a central ring, all in close contact with each other. Only the Q_Y and Q_X transition dipole moments are taken into account. Calculation of the spectra of such a system requires diagonalization of a 320×320 Hamiltonian; consequently, accounting for even more transition dipole moments would render the program practically unusable. In Figure 7, the results

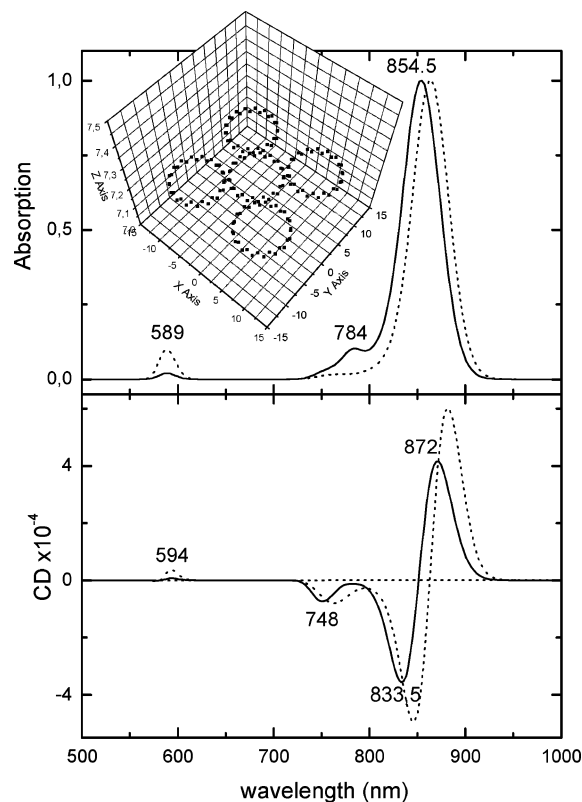


Figure 7. Modeled absorption (top) and CD (bottom) spectra of an aggregate of BChl rings. With dotted lines, the spectra of one ring of BChls are overlaid. Only the Q_Y and Q_X transitions are taken into account. In the insert (tilted by a few degrees), the arrangement of the BChl rings is presented.

of such a calculation are presented. The Q_Y absorption spectrum shifts significantly to the blue (to 854 nm) and displays a large shoulder at 784 nm, while the CD signal follows the shift of the absorption and loses some intensity without any further changes in the shape. In the Q_X region, both the absorption and CD signals become approximately five times smaller in intensity, however, they are very stable in terms of shape. These results show that aggregation of LH complexes in a sample must have strong effects in the Q_Y absorption, and thus it should be easily detected.

Discussion/Conclusions

In this modeling study, we have tried to explain the absorption and CD spectra of LH1 complexes from *Rba. sphaeroides* and *Rsp. rubrum*, with different carotenoid content. By using these spectra as a starting point and on the basis of our knowledge of LH2 structures, we create a “model” LH1 ring and we subsequently vary the position of its carotenoid bands in order to simulate the changes between the measured samples. It is important to note here that we are not trying to calculate the spectra of a specific complex, and therefore, we do not attempt to simulate precisely every single band present in a certain experimental spectrum. Such an effort is being made in the companion paper,⁴⁴ where a single complex is chosen and its absorption and CD signals are modeled with great precision. In this study, we are mainly looking for trends and try to identify those interactions that dominate the spectra. Therefore, there are many differences between measurements, presented in detail in the companion paper,⁴⁴ and calculations. Most obvious are the discrepancies in the Soret region of all the complexes. These are mainly due to other BChl transitions that absorb around the

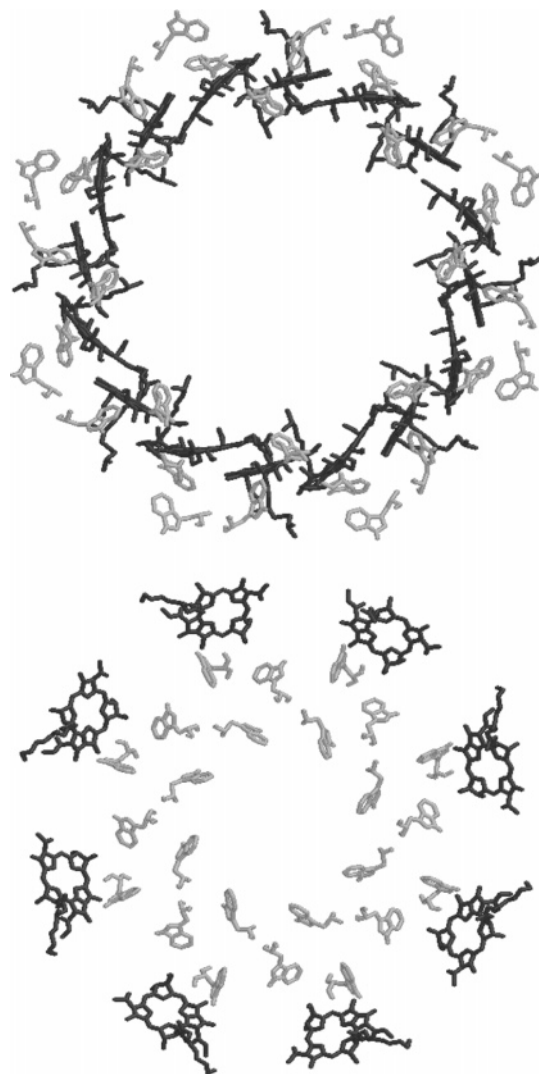


Figure 8. B850 (top) and the B800 (bottom) rings of BChls from *Rsp. molischianum* LH2 complex. In light gray, the tryptophans (trp) are shown. Four rings of trp surround the B850 BChls, while the B800 BChls enclose three rings of trp.

same wavelengths; the N transition, for example, mixes with the Soret so much that it is not always possible to clearly identify them in the BChl absorption spectrum,⁴⁹ and thus the positions and intensities of the individual bands cannot be accurately assigned. Moreover, interactions with the protein that are not accounted for in the modeling, are likely to affect the absorption and CD spectra of the Soret region. We have seen that interactions with higher transitions can affect the spectra significantly. Moreover, we know from the structures of LH2 complexes that there are rings of tryptophans (trp), belonging to the apoproteins, that are surrounding the B850 and B800 BChls rings (Figure 8). Tryptophans have absorption bands between 250 and 300 nm and display very strong CD signals;⁵⁰ they are, therefore, the most likely to interact with the Soret region. By creating such rings of trp transition dipole moments in close contact with the BChls, with site energies between 260 and 290 nm, we can easily show that they significantly affect the Soret bands (Figure 9). We also observe a small shift to the red of the Q_Y bands by approximately 2 nm. For modeling the entire LH1 spectra, we have not included any protein interaction, nor any higher BChl transitions, to make our calculations simpler; thus, big discrepancies in the blue are expected and are very well justified.

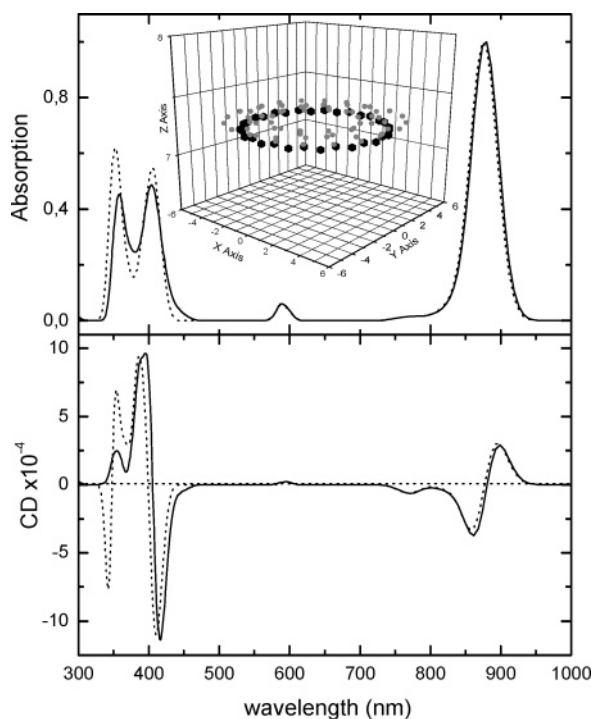


Figure 9. Modeled absorption (top) and CD (bottom) spectra of a BChl ring, with four rings of trp in close contact with the BChls (positions shown in the insert: black, BChls; grey, trp). The trp are given site energies between 260 and 290 nm and a dipole moment of around 3.9 D. With dotted lines, the spectra of a ring of BChls only are overlaid. The parameters for the BChls are the same as in Table 1.

The carotenoid signals of the measured complexes also differ significantly from the ones calculated here (for a detailed account of the measured spectra, see companion paper).⁴⁴ As mentioned earlier, in the modeling program, we assume a BChl/carotenoid ratio of 2:1. Moreover, we assign spectroscopic properties to the carotenoids that are in general agreement with the spectra of both *Rba. sphaeroides* and *Rsp. rubrum* without putting any effort on modeling the specific features of each complex in that region like fine structure or intensity. By default, it is in this way impossible to get a precise fit between model and experiment.

Another cause of discrepancies between model and experiment, particularly for the mutant species, is that, for the calculation of the spectra presented here, the BChl dipole moments are not rotated further once the carotenoids are added. In this way, we show clearly the effect of carotenoids on the Q_Y region. All the changes on the Q_Y signals that can be seen in the consecutive calculated spectra are due solely to the electronic interaction with the carotenoids. In reality, it is very possible that the carotenoids affect also the orientation of the BChls and thus cause rotation of their dipole moments. Changes in the binding site of the B850 BChls in the LH2 of *Rba. sphaeroides*, depending on the existence or not of the carotenoids and on their chemical nature, have been reported in the past.⁵¹ These are rendered responsible for a small, but global reorganization of the B850 BChls. By performing these rotations, we can get better fits for the individual species and reproduce features such as the exact signature of the CD signal and the shifts of the absorption. For example, by changing the rotation of the Q_Y transition dipole moments of the α -BChls around the pigment's z -axis by only 5°, we obtain the same signature in the Q_Y CD signal as the one observed experimentally (Figure 10). A better example, where the entire spectrum is modeled in detail, can be found in the companion paper⁴⁴

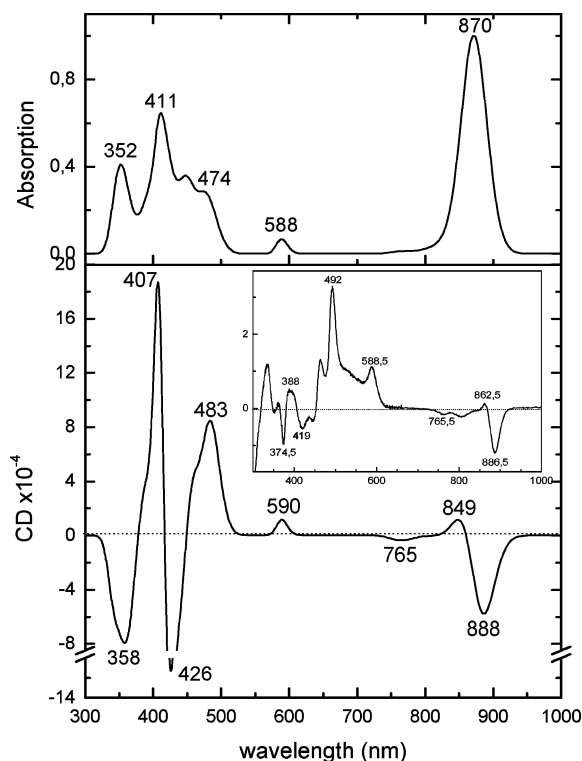


Figure 10. Modeled absorption (top) and CD (bottom) spectra of an LH1 ring with 16-fold symmetry containing a carotenoid that absorbs further to the blue (neurosporene-like). The parameters used for the modeling are the same as for Figure 5A, with an extra rotation of the α -BChl Q_Y by 5° around the pigment's z -axis. The insert shows the measured CD signal of a mutant from *Rba. sphaeroides* LH1 (WTW), which contains the carotenoid neurosporene. For more details on measured spectra, see companion paper.⁴⁴

for the WT LH1 complex from *Rsp. rubrum*. However, as mentioned several times, the exact reproduction of the measured spectra is not the point of this work. On the other hand, we are very interested in seeing how higher transitions affect the NIR region and in explaining the nonconservativity and small intensity of the Q_Y CD signal.

The first thing we observe when adding the Soret transitions is the shift of the Q_Y site energy to the red. When we model only the Q_Y , Q_X regions, the BChl Q_Y bands are situated several nanometers to the blue compared to the calculations that include the Soret transitions. By adding these transitions, and specifically the B_Y , the Q_Y bands are significantly red-shifted; we are thus able to use site energies for the Q_Y that are closer to those of the monomeric BChls and still produce bands at the desired wavelength (around 870 nm). Hence, the rather big discrepancy between the Q_Y site energies of monomeric BChls and the values used for modeling the NIR region of a LH ring^{24,39,49} is partly compensated by introducing the interaction with the BChls' Soret dipole moments and the assumed shift in site energy and is, therefore, not just an effect of the protein environment. The Soret site energies are also red-shifted with respect to what is observed for monomeric BChls;³⁹ this time, the effect of the interaction with the protein is probably larger because the Soret bands are energetically very close to the protein transitions. The B_X transition alone has no effect on the position of the Q_Y site energies; it can, however, significantly affect the shape of the Q_Y CD signal.

The very small intensity of the LH1 CD signal in the Q_Y region arises at once when we increase the size of the symmetry and the ring size with respect to the LH2 ring. This can be understood as follows: Q_Y interactions between two pigments

that are a quarter of a ring apart are responsible for much of the CD signal's intensity in that region; because their Q_Y dipole moments are perpendicular to each other, they induce larger rotational strength than nearest neighbors, whose dipole moments are almost parallel. By increasing the symmetry number and the ring size, we separate the two pigments with perpendicular dipoles more, thus weakening their interaction. Combined with small rotations of the transition dipole moments, this leads to the reproduction of the weak CD signal of the Q_Y region in LH1.

The main and most important conclusion we can draw from this modeling procedure is that the strong nonconservativity of the Q_Y CD signal is caused to a large extent by the interaction with the carotenoids. When no carotenoids are present, the CD signals in the NIR are mainly conservative. A small loss of the conservativity can occur due to the Soret transitions (see companion paper for an example),⁴⁴ but not to the extent that is seen, for example, in the WT LH1 spectrum of *Rba. sphaeroides*. Once carotenoids are introduced, the conservative nature of the Q_Y CD signal is distorted. In fact, we observe that the extent of the interaction with the Q_Y depends on the value of the carotenoid site energies: redder carotenoids affect the Q_Y more. Because the position of the carotenoid bands change with the length of the carotenoid conjugated chain,⁴⁸ we conclude that longer, and therefore redder, carotenoids have a bigger effect on the nonconservativity of the Q_Y CD signal.

The revelation of the structures of LH2 complexes opened the way for a thorough understanding of their CD spectra; many aspects of ring structures and their excitonic CD signals could be elucidated.^{19,20,24,35,37} In this work, we expand our knowledge by using the tools we acquired from previous research in order to understand the spectra of similar complexes with unknown structures. For the first time, interactions between all the pigments that comprise the LH rings are accounted for, and the absorption and CD signals at the near-UV, visible, and NIR spectral range are calculated simultaneously. This way, we can identify the importance of the interaction between each transition and each pigment group. Finally, we are able to model and explain absorption and CD spectra of LH1 antennae whose signals remained a mystery for years; although these signals seem peculiar at first sight, we have shown that they arise from complexes that have similar structures and follow the same excitonic model as LH2.

References and Notes

- (1) Fleming, G. R.; van Grondelle, R. *Phys. Today* **1994**, *47*, 48–55.
- (2) Pullerits, T.; Sundström, V. *Acc. Chem. Res.* **1996**, *29*, 381–389.
- (3) Hu, X. C.; Schulten, K. *Phys. Today* **1997**, *50*, 28–34.
- (4) Hu, X. C.; Damjanovic, A.; Ritz, T.; Schulten, K. *Proc. Natl. Acad. Sci. U.S.A.* **1998**, *95*, 5935–5941.
- (5) Sundstrom, V.; Pullerits, T.; van Grondelle, R. *J. Phys. Chem. B* **1999**, *103*, 2327–2346.
- (6) Deisenhofer, J.; Epp, O.; Miki, K.; Huber, R.; Michel, H. *Nature* **1985**, *318*, 618–624.
- (7) Karrasch, S.; Bullough, P. A.; Ghosh, R. *EMBO J.* **1995**, *14*, 631–638.
- (8) McDermott, G.; Prince, S. M.; Freer, A. A.; Hawthornthwaite-Lawless, A. M.; Papiz, M. Z.; Cogdell, R. J.; Isaacs, N. W. *Nature* **1995**, *374*, 517–521.
- (9) Koepke, J.; Hu, X. C.; Muenke, C.; Schulten, K.; Michel, H. *Structure* **1996**, *4*, 581–597.
- (10) Fritzsche, G.; Koepke, J.; Diem, R.; Kuglstatter, A.; Baciou, L. *Acta Crystallogr., Sect. D* **2002**, *58*, 1660–1663.
- (11) Roszak, A. W.; Howard, T. D.; Southall, J.; Gardiner, A. T.; Law, C. J.; Isaacs, N. W.; Cogdell, R. J. *Science* **2003**, *302*, 1969–1972.
- (12) Papiz, M. Z.; Prince, S. M.; Howard, T. D.; Cogdell, R. J.; Isaacs, N. W. *J. Mol. Biol.* **2003**, *326*, 1523–1538.
- (13) Sauer, K.; Cogdell, R. J.; Prince, S. M.; Freer, A.; Isaacs, N. W.; Scheer, H. *Photochem. Photobiol.* **1996**, *64*, 564–576.
- (14) Alden, R. G.; Johnson, E.; Nagarajan, V.; Parson, W. W.; Law, C. J.; Cogdell, R. G. *J. Phys. Chem. B* **1997**, *101*, 4667–4680.
- (15) Krueger, B. P.; Scholes, G. D.; Fleming, G. R. *J. Phys. Chem. B* **1998**, *102*, 5378–5386.
- (16) Tretiak, S.; Middleton, C.; Chernyak, V.; Mukamel, S. *J. Phys. Chem. B* **2000**, *104*, 9540–9553.
- (17) Tretiak, S.; Middleton, C.; Chernyak, V.; Mukamel, S. *J. Phys. Chem. B* **2000**, *104*, 4519–4528.
- (18) Linnanto, J.; Korppi-Tommola, J. E. I.; Helenius, V. M. *J. Phys. Chem. B* **1999**, *103*, 8739–8750.
- (19) Koolhaas, M. H. C.; van der Zwan, G.; Frese, R. N.; van Grondelle, R. *J. Phys. Chem. B* **1997**, *101*, 7262–7270.
- (20) Koolhaas, M. H. C.; Frese, R. N.; Fowler, G. J. S.; Bibby, T. S.; Georgakopoulou, S.; van der Zwan, G.; Hunter, C. N.; van Grondelle, R. *Biochemistry* **1998**, *37*, 4693–4698.
- (21) Pullerits, T.; Chachisvilis, M.; Sundstrom, V. *J. Phys. Chem.* **1996**, *100*, 10787–10792.
- (22) Novoderezhkin, V.; Monshouwer, R.; van Grondelle, R. *J. Phys. Chem. B* **1999**, *103*, 10540–10548.
- (23) Monshouwer, R.; Abrahamsson, M.; van Mourik, F.; van Grondelle, R. *J. Phys. Chem. B* **1997**, *101*, 7241–7248.
- (24) Georgakopoulou, S.; Frese, R. N.; Johnson, E.; Koolhaas, M. H. C.; Cogdell, R. J.; van Grondelle, R.; van der Zwan, G. *Biophys. J.* **2002**, *82*, 2184–2197.
- (25) Bahatyrova, S.; Frese, R. N.; Siebert, C. A.; Olsen, J. D.; van der Werf, K. O.; van Grondelle, R.; Niederman, R. A.; Bullough, P. A.; Otto, C.; Hunter, C. N. *Nature* **2004**, *430*, 1058–1062.
- (26) Bahatyrova, S.; Frese, R. N.; van der Werf, K. O.; Otto, C.; Hunter, C. N.; Olsen, J. D. *J. Biol. Chem.* **2004**, *M313039200*.
- (27) Iida, K.; Inagaki, J. I.; Shinohara, M.; Suemori, Y.; Ogawa, M.; Dewa, T.; Nango, M. *Langmuir* **2005**, *21*, 3069–3075.
- (28) Scheuring, S.; Francia, F.; Busselez, J.; Melandri, B. A.; Rigaud, J. L.; Levy, D. *J. Biol. Chem.* **2004**, *279*, 3620–3626.
- (29) Scheuring, S.; Levy, D.; Rigaud, J. L. *Biochim. Biophys. Acta* **2005**, *1712*, 109–127.
- (30) Hu, X.; Schulten, K. *Biophys. J.* **1998**, *75*, 683–694.
- (31) Pandit, A.; van Stokkum, I. H. M.; Georgakopoulou, S.; van der Zwan, G.; van Grondelle, R. *Photosynth. Res.* **2003**, *75*, 235–248.
- (32) Parkes-Loach, P. S.; Sprinkle, J. R.; Loach, P. A. *Biochemistry* **1988**, *27*, 2718–2727.
- (33) Visschers, R. W.; Nunn, R.; Calkoen, F.; van Mourik, F.; Hunter, C. N.; Rice, D. W.; van Grondelle, R. *Biochim. Biophys. Acta* **1992**, *1100*, 259–266.
- (34) Germeroth, L.; Lottspeich, F.; Robert, B.; Michel, H. *Biochemistry* **1993**, *32*, 5615–5621.
- (35) Georgakopoulou, S.; van Grondelle, R.; van der Zwan, G. *Biophys. J.* **2004**, *87*, 3010–3022.
- (36) Koolhaas, M. H. C.; van Mourik, F.; van der Zwan, G.; van Grondelle, R. *J. Lumin.* **1994**, *60–I*, 515–519.
- (37) Koolhaas, M. H. C.; van der Zwan, G.; van Grondelle, R. *J. Phys. Chem. B* **2000**, *104*, 4489–4502.
- (38) Koolhaas, M. H. C.; van der Zwan, G.; van Mourik, F.; van Grondelle, R. *Biophys. J.* **1997**, *72*, 1828–1841.
- (39) Scherz, A.; Rosenbach-Belkin, V.; Fisher, J. R. E. In *Chlorophylls*; Scheer, H., Ed.; CRC Press: Boca Raton, 1991; pp 237–268.
- (40) Georgakopoulou, S.; Cogdell, R. J.; van Grondelle, R.; van Amerongen, H. *J. Phys. Chem. B* **2003**, *107*, 655–658.
- (41) Mukamel, S. In *Principles of Nonlinear Optical Spectroscopy*; Lapp, M.; Nishizawa, J.-I.; Snively, B. B.; Stark, H.; Tam, A. C.; Wilson, T., Eds.; Oxford University Press: New York, Oxford, 1995; pp 209–259.
- (42) Brunisholz, R. A.; Zuber, H. *J. Photochem. Photobiol., B* **1992**, *15*, 113–140.
- (43) Cogdell, R. J.; Scheer, H. *Photochem. Photobiol.* **1985**, *42*, 669–678.
- (44) Georgakopoulou, S.; van der Zwan, G.; Olsen, J. D.; Niederman, R. A.; Hunter, C. N.; van Grondelle, R. **2006**, *110*, 3354–3361.
- (45) Scholes, G. D.; Gould, I. R.; Cogdell, R. J.; Fleming, G. R. *J. Phys. Chem. B* **1999**, *103*, 2543–2553.
- (46) Pullerits, T.; Hess, S.; Herek, J. L.; Sundstrom, V. *J. Phys. Chem. B* **1997**, *101*, 10560–10567.
- (47) Novoderezhkin, V.; van Grondelle, R. *J. Phys. Chem. B* **2002**, *106*, 6025–6037.
- (48) Britton, G. In *Carotenoids*; Britton, G.; Liaaen-Jensen, S.; Pfander, H., Eds.; Birkhäuser: Basel, Boston, Berlin, 1995; Vol. 1B (Spectroscopy), pp 13–62.
- (49) Weiss, C. In *The Porphyrins*; Dolphin, D., Ed.; Academic Press: New York, San Francisco, London, 1978; Vol. III, pp 211–223.
- (50) Gasyimov, O. K.; Abduragimov, A. R.; Yusifov, T. N.; Glasgow, B. J. *Anal. Biochem.* **2003**, *318*, 300–308.
- (51) Gall, A.; Cogdell, R. J.; Robert, B. *Biochemistry* **2003**, *42*, 7252–7258.